Proceedings of ISFOG 2025
5TH INTERNATIONAL SYMPOSIUM ON
FRONTIERS IN OFFSHORE GEOTECHNICS
Nantes, France | June 9-13 2025
© 2025 the Authors
ISBN 978-2-85782-758-0

Centrifuge modelling of shared ring anchors for floating wind turbines subjected to cyclic loading in clay

L. Huang
University of California Davis, Davis, United States of America

K. Coughlan
University of Massachusetts Amherst, Amherst, United States of America

A. Martinez*
University of California Davis, Davis, United States of America

D. Wilson
University of California Davis, Davis, United States of America

C. Aubeny
University of Texas A&M, College Station, United States of America

S. Arwade, D. DeGroot
University of Massachusetts Amherst, Amherst, United States of America

R. Beemer
Virginia Tech University, Blackburg, United States of America

amart@ucdavis.edu (corresponding author)

ABSTRACT: Shared configurations can significantly reduce the number of anchors required for floating offshore wind projects, potentially increasing their economic competitiveness. However, this configuration results in interaction between the loads transferred to the anchor by each of the turbines. The ring anchor has emerged as a viable anchor alternative due to its high capacity, small size, and symmetric shape. This investigation provides the results of cyclic centrifuge load tests on ring anchors embedded in normally consolidated clay performed at an acceleration of 70g. The tests characterize the cyclic stability of the anchors under expected and extreme cyclic loads. Three actuators connected to each anchor via taut lines apply cyclic loads to simulate the load conditions generated by three wind turbines. In addition, in-flight T-bar soundings provide characterization of the strength of the deposits. The results show the behavior of the ring anchors under expected environmental loads, exhibiting small displacements. However, extreme cyclic loads can lead to significant displacement due to the summative interactions between the vertical components of the three applied loads. The results show the possible benefits of shared anchor configurations in maintaining stability while reducing the number of required anchors.

Keywords: Shared anchors; centrifuge modelling; cyclic loading; clay

1 INTRODUCTION

A significant portion of offshore wind energy resources are located in deep water regions, where installing wind turbines on fixed foundations like monopiles or jacket structures is physically or economically unfeasible. For example, in the United States, it is estimated that 65% of the offshore wind energy resources are in locations with water depths greater than 60 m (Lopez et al. 2022). In these locations, floating offshore wind turbines (FOWTs) that maintain positioning with mooring systems and subsea anchors are needed. Considering that the foundations for FOWTs typically account for 25% to 35% of the total construction cost (Lee et al. 2020), reducing the number of anchors per turbine by means of shared configurations can significantly improve the economic competitiveness of floating offshore wind (Fontana et al. 2018). In this configuration, each anchor is typically shared between three FOWTs (Figure 1), resulting in a reduction of the number of anchors by up to a factor of three.

Deeply embedded ring anchors have emerged as an efficient alternative to existing solutions such as piles, suction caissons, and drag anchors due to their more compact size, facilitating transport to the project site and reducing material usage (Lee et al. 2020).

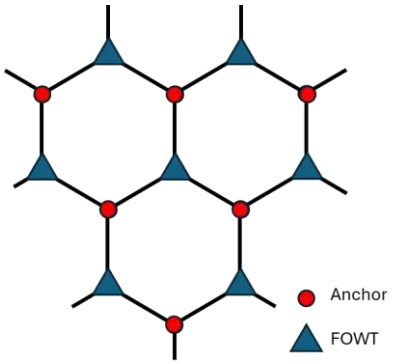

Figure 1. Schematic of a shared anchor configuration

Ring anchors have a circular cross section and aspect ratios (i.e., length to diameter) of one to two, as shown in Figure 2, and are designed to be installed by hammer or impact driving with a retractable follower. The deep embedment of the ring anchors makes them compact, resulting in higher efficiencies in terms of unit capacity per unit material. Previous centrifuge experiments in sand and clay have characterized their behavior in monotonic loading conditions with different line loading angles (Huang et al. 2024; Huang et al. 2025). Due to the smaller vertical capacity of the ring anchors in comparison to their horizontal capacity and the additive contribution of the loads on the multiple lines in shared configurations (Fontana et al. 2018), the most likely failure mode of the ring anchors is expected to be governed by loss of embedment due to vertical displacements.

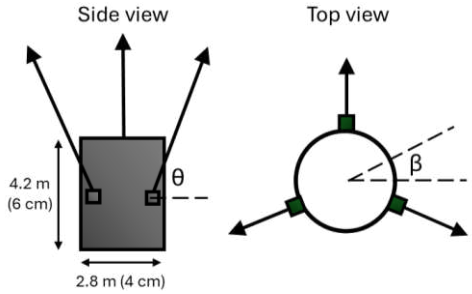

Figure 2. Schematic of a shared ring anchor. The dimensions in parentheses are in model scale.

Anchors for FOWTs are subjected to environmental loads due to wind, wave, and tide action. These loads have both static and cyclic components. In shared configurations, the loads applied by the three individual FOWT's determine the magnitude, inclination (θ in Figure 2), and out of plane direction (β in Figure 2) of the resultant force acting on the subsea anchor. Therefore, anchors need to be designed to resist loads at various inclination angles even when subjected to stress reversals.

This paper presents results of two cyclic load tests on ring anchors shared by three FOWTs performed in a geotechnical centrifuge. The anchors were embedded to a depth of six anchor diameters (D) in a deposit of normally consolidated clay and loaded with lines with a taut angle of 70°. Both tests had the same static load magnitude but differed in the amplitude of cyclic load.

2 MATERIALS AND METHODS

2.1 Centrifuge testing and soil model

Anchor load tests were performed at the Center for Geotechnical Modeling (CGM) at the University of California Davis in a 9-m radius centrifuge at an acceleration of 70g. The tests were performed in a flexible shear beam container with model dimensions of 1.65 m, 0.79 m, and 0.60 m in length, width, and depth, respectively. Unless noted otherwise, all the quantities reported are in prototype scale.

The tests were performed in a deposit of kaolin clay, which has a median particle size of 4 μm, liquid limit of 37%, plastic limit of 23%, compression index of 0.181, recompression index of 0.045, coefficient of consolidation (C_V) of 0.018 cm^2/s at a vertical effective stress of 80 kPa, and specific gravity of 2.58. The clay deposit was initially consolidated at 1g in a press fitted with a rectangular plate to reduce the centrifuge spinning time. The clay model was consolidated in six layers, forming a consolidated deposit with a depth of 31.5 m (0.45 m in model scale). A layer of geotextile fabric was embedded at a depth of 14 m to reduce the consolidation time in the centrifuge. Cutouts were included in the fabric layer to allow the anchors, lines, and T-bars to reach the desired depths. The stress applied by the press was selected to match the overburden stress at 70g at the bottom of each of the six sublayers. This resulted in a deposit with an OCR smaller than 1.5 at depths greater than 4.9 m. However, this consolidation stress created a shallow layer with high OCR values, as described in Huang et al. (2025).

In-flight T-bar soundings were performed at 70g to characterize the undrained shear strength (s_u) of the clay deposit. The results yielded the s_u profiles presented in Figure 3 using a T-bar factor of 12 (DeJong et al. 2011), showing a steady increase with depth at a rate of 4.4 kPa/m in both soundings. The s_u profiles show elevated values at depths smaller than 2 m due to the presence of the highly OC crust, which is not considered to influence the anchors' behavior due to their much greater embedment.

The anchors had a diameter (D) of 2.8 m (4 cm in model scale) and a length (L) of 4.2 m (6 cm in model scale) (Figure 2), resulting in an L/D of 1.5. The anchor pad eye was at a distance equivalent to 0.69*L form the bottom of the anchor. Both load tests were performed on anchors embedded to a depth to the

anchor top of six D, equivalent to 18.9 m to the anchor mid height. Both tests were performed on anchors with three lines with a taut angle from the horizontal (i.e., θ) of 70°. The anchors were installed at 1g using an installation tool that embeds the cables at the desired θ, as described in Huang et al. (2024). Cyclic load-controlled tests were performed using independently controlled electromechanical actuators, as shown in Figure 4, where the actuators are connected to an embedded anchor by means of wire rope cables. The load cycles were applied at a frequency of 0.1 hz. Prior to this investigation, an actuator was used to perform displacement-controlled monotonic tests, as discussed in Section 3.1. Load cells and linear potentiometers were connected on each of the three lines to monitor their force and displacement. During the cyclic load tests, Line A was at a β angle of 0° (east), line B at a β of 120°, and line C at a β angle of -120°.

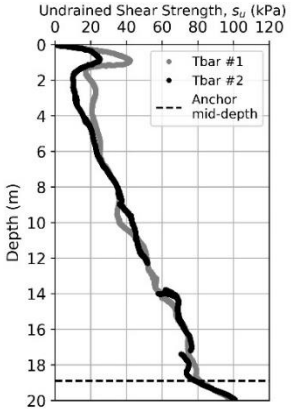

Figure 3. Undrained shear strength profiles from T-bar soundings in the clay model

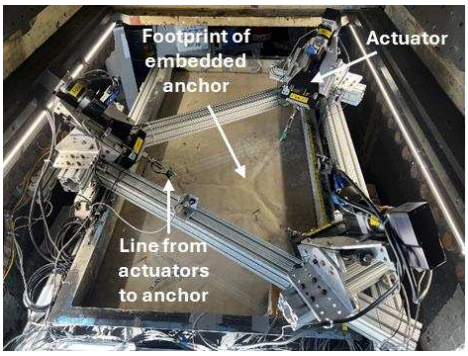

Figure 4. Photograph of the actuator system for applying cyclic loads to shared anchors in the centrifuge

2.2 Applied cyclic loads

To provide realistic cyclic loading parcels, dynamic FOWT simulations were run in OpenFAST using the the IEA Wind 15 MW offshore reference turbine with the University of Maine's VolturnUS-S semisubmersible platform (Allen 2020). An IEC survival case (i.e., SLC / DLC 1.1) was considered for the first centrifuge test (i.e., referred to as Load level 1), which corresponds to extreme wind and wave conditions corresponding to a 500-year return period in wind speed, wave height, and wave period (IEC 2019). Conditions for a deep-water site off the coast of California were considered for a taut angle of 60°, which is slightly lower than that in the centrifuge tests. In the simulations, each anchor receives loads from three FOWTs at 0° (east), 120°, and -120°. The Load level 1 corresponds to a ratio of applied mean load (Q_m) to vertical anchor capacity (Q_v) of about 0.38 and cyclic amplitude (Q_c) to Q_v ratios that range from 0.01 to 0.08. More details on the mooring system, anchor loads, and cyclic analysis can be found in Davis (2023) and Couhlan (2024).

The results of these simulations were used to develop idealized loading packets with a normalized constant static load but increasing normalized cyclic amplitude from 0.044 for 50 cycles to 0.058 for 50 cycles to 0.073 for 15 cycles. It took an average 3.5 hours in model time (t) (715 days in prototype time) to apply all nine packets. The Randolph (2003) method yields a normalized time of 70.8, indicating that the excess pore pressures developed in the first cycles fully dissipated by the end of the test. Nine packets were applied, where the out of plane angle (i.e., β) was changed between packets from -90° (south), to -45°, 0° (east), 45°, and 90° in the first five packets and then returned to 45°, 0°, -45°, and -90°. A higher load scenario was considered (referred to as Load level 2) where the applied Q_m/Q_v was kept at 0.38 but the Q_c/Q_v amplitudes were multiplied by a factor of three. Figure 5 shows the normalized loads applied to each line for the nine packets.

3 RESULTS

3.1 Monotonic pullout tests

Monotonic tests in a deposit composed of the same clay and prepared in the same manner as described in Section 2.1 were performed as part of a previous centrifuge testing campaign, as described in Huang et al. (2025). The results of tests at 90° (i.e., vertical), which were used to determine Q_V for normalizing the loads, and at 70°, which corresponds to the same taut line angle used in the cyclic shared anchor tests, are presented in Figure 6. The monotonic results indicate a rapid increase in load up to displacements between 0.2 and 0.3 m, followed by a plateau. The test at 90° mobilized a slightly smaller capacity, determined at a displacement equivalent to 0.2D, of 3.7 MN, while the test at 70° mobilized a capacity of 4.1 MN. However, the vertical force component of the test at 70° is 3.85

MN, which is close to Q_V. The small differences in capacity indicate limited interactions between the axial and vertical loads in this range of loading angles.

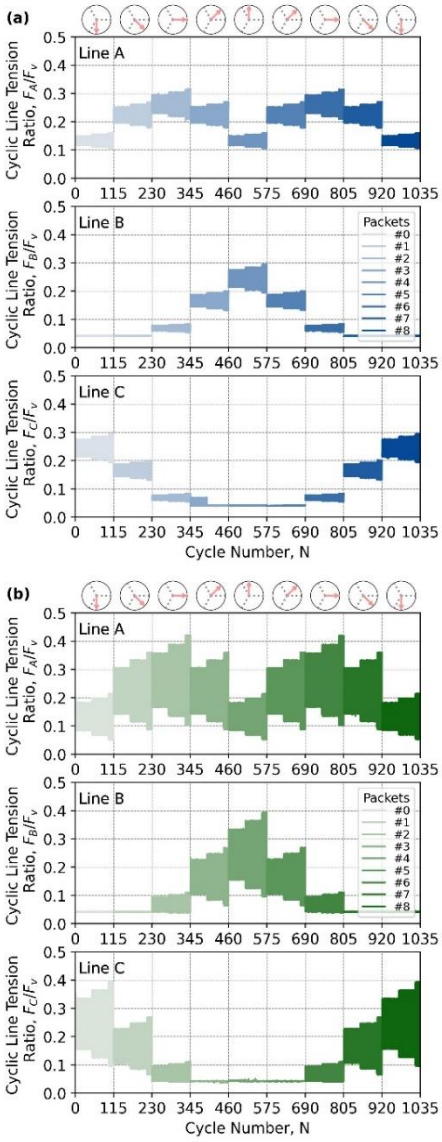

Figure 5. Loads applied to ring anchors during tests with (a) Load level 1 and (b) Load level 2 (the schematics on the top of each figure show the resultant β in each load packet)

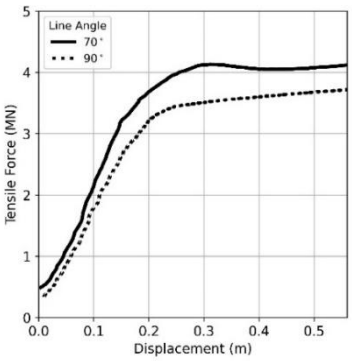

Figure 6. Results of monotonic pullout tests on ring anchors embedded at 6D with lines at 90° (vertical) and 70°

3.2 Cyclic tests in clay

The anchor subjected to Load level 1 experienced resultant force that had a constant mean load normalized by Q_V of 0.38 and cyclic amplitude normalized Q_V of 0.044 to 0.058 to 0.073, which are achieved at different β angles by controlling each line load independently, as shown in Figure 5a. Figure 7a shows the total loads applied to the anchor in each load packet (note that packets 1 and 9, 2 and 8, 3 and 7, and 4 and 6 overlap).

As a result of these applied loads, anchor displacements were accumulated, as shown in Figure 7b, where the anchor's initial location is set at the origin of the graph. The first load packet induces a significant amount of displacement which has its greatest magnitude in the y direction (about 0.26 m), in allignment with the β angle in this packet, while the anchor experiences about 0.08 m in vertical displacement (Figure 7b). With increasing load packets, horizontal displacements continue to accumulate with their directions largely coinciding with the β of the specific load packet. At the end of packet 9, the anchor's displacement in the horizontal plane is small due to the changes in β, leading to an x displacement (d_x) of 0 m and y displacement (d_y) of 0.13 m. In contrast, the vertical displacements (d_z) continue to accumulate throughout all load packets, leading to a final displacement of about 0.14 m.

The accumulated displacements are greater in the initial load packets than in the latter ones. Particularly, packets 1 to 5 lead to about 0.12 m of vertical displacements, while packets 6 to 9 lead to a modest increase to 0.14 m of vertical displacement. This indicates that the soil hardens as a result of the multiple cyclies applied. This could be related to the dissipation of pore pressures during the period of load application.

The test performed with Load level 2 exhibited similar trends as those with Load level 1, with the main difference being the larger displacements due to the greater loads. Specifically, 0.30 m of d_z were accumulated by the end of the test, while the total d_x and d_y are of about 0.20 m. Greater displacements were accumulated during the initial five load packets, contributing 0.26 m of d_z in comparison to a modest increase to 0.30 m due to packets six to nine, in a similar fashion as the test with Load level 1. All packets induced greater displacements in the horizontal direction than in the vertical one, but a large portion of them were reversed due to the change in β between packets. It is interesting noting that while the normalized mean load was kept constant, an increase in cyclic load led to an increase of 210% in the accumulated vertical displacements.

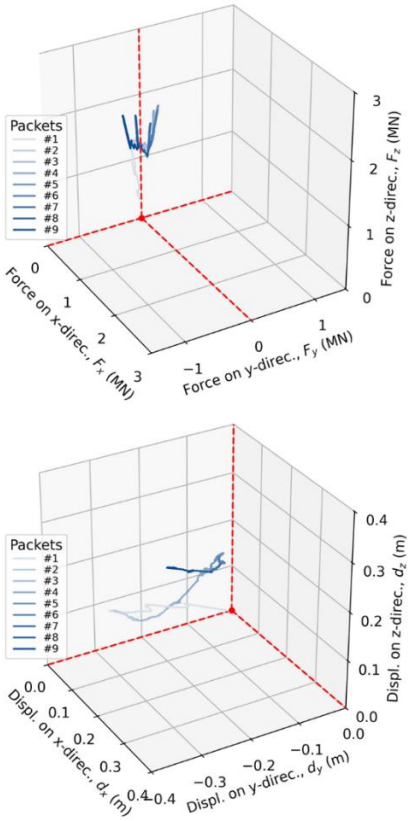

Figure 7. Results of tests with load level 1: 3D evolution of (a) applied loads and (b) resulting displacements

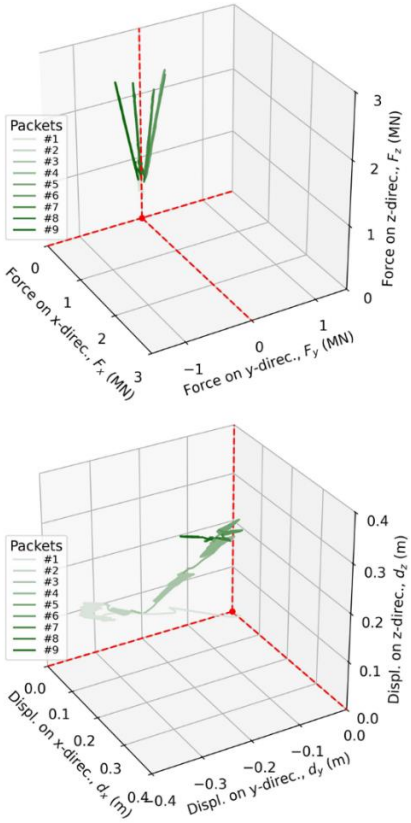

Figure 8. Results of tests with load level 2: 3D evolution of (a) applied loads and (b) resulting displacements

A comparison of the accumulated displacements (d_{ACC}) in each packet as a function of cycle number is presented in Figure 9 for the three lines connected to each anchor. It is noted that d_{ACC} is set to zero at the beginning of each packet. The figure shows the greater displacements in all lines in the test with Load level 2. The greater displacements in the first five load packets for both tests are evident in the figure, clearly showing that once the β is reversed to a direction that has already been loaded in packets 6 to 9 the accumulated displacements are small in all lines. The results also show that the variation in the displacement between different lines in each packet, which is a result of the load applied to each line to achieve the target mean and cyclic load and β angle. For example, the d_{acc} are initially smallest in line B due to the smaller applied load magnitudes (Figures 5a and b), but increase in packets 3, 4 and 5 due to the increase in the applied load. Similarly, the d_{acc} in line C reduces from packet 1 to 2 due to the decrease in load amplitude. Despite the influence of load magnitude, the d_{acc} show a decrease as loading continues due to the progressive hardening of the clay.

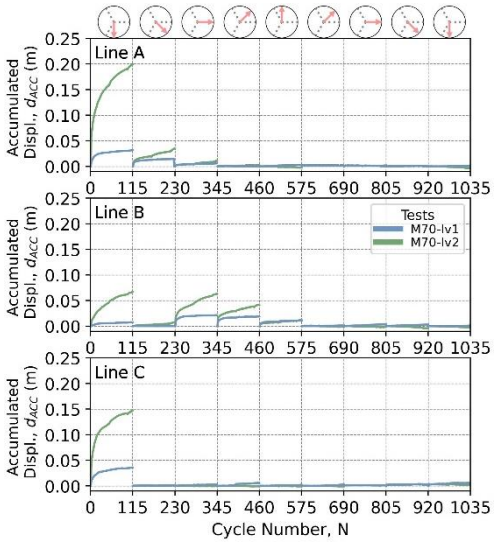

Figure 9. Comparison of accumulated line displacements per packet in tests performed with Load levels 1 and 2

4 CONCLUSIONS

This paper presents the results of centrifuge tests on shared ring anchors embedded in a normally consolidated clay deposit. Two load tests were performed on anchors loaded by three individually controlled actuators that simulate the loads applied in a shared configuration. The applied loads were based on simulations using the OpenFAST program. Each test involved nine load packets with changing direction in the horizontal plane. In-flight T-bar soundings characterize the undrained shear strength of the soil.

The tests indicate that increasing the cyclic amplitude of the loads while maintaining the mean load constant results in greater anchor displacements, as expected. Particularly, increasing the cyclic amplitude by a factor of 3.0 led to an increase in the vertical accumulated displacements by a factor of 2.1. During each packet, the horizontal displacements were greater than the vertical ones. However, due to the changes in total force horizontal direction between packets (i.e., from -90 in packet 1 to 90 in packet 5 to -90 in packet 9), the horizontal displacements were small by the end of the test. In contrast, the vertical displacements continued to accumulate, resulting in some loss of embedment. Anchor displacements were greater in the initial five packets in both tests, with very small displacements in the packets that loaded the anchor in a horizontal direction that had been loaded before. This behavior suggests hardening of the material which is likely due to the dissipation of pore pressures during the long period of load application. The results of the centrifuge tests indicate that under a single out of plane direction, the horizontal anchor displacements are likely to be greater, but the vertical displacements are likely to govern failure in the long term where the out of plane angle can change between different loading events (i.e., storms). However, the effect of other factors such as the line angle and clay strength and coefficient of consolidation should also be considered.

AUTHOR CONTRIBUTION STATEMENT

L. Huang: Formal Analysis, Investigation, Methodology, Validation, Visualization, Writing–reviewing and editing. **K. Coughlan**: Formal Analysis, Investigation, Writing–reviewing and editing. **A. Martinez**: Conceptualization, Funding acquisition, Investigation, Methodology, Project Administration, Supervision, Writing–original draft. **D. Wilson**: Methodology, Resources, Writing–reviewing and editing. **C. Aubeny**: Conceptualization, Funding acquisition, Writing–reviewing and editing **S. Arwade**: Conceptualization, Funding acquisition, Writing–reviewing and editing. **D. DeGroot**: Conceptualization, Funding acquisition, Writing–reviewing and editing. **R. Beemer**: Conceptualization, Funding acquisition, Writing–reviewing and editing.

ACKNOWLEDGEMENTS

The authors would like to acknowledge the contributions of Junho Lee, Chad Justice, and Tom Kohnke. This material is based upon work supported by National Science Foundation (NSF) under Cooperative Agreement No. CMMI-1936939. The UC Davis Center for Geotechnical Modeling is supported under the grant CMMI-1520581. Any opinions, findings, conclusions, or recommendations expressed in this material are those of the author(s) and do not necessarily reflect those of the NSF.

REFERENCES

Allen, C., Viscelli, A., Dagher, H., Goupee, A., Gaertner, E., Abbas, N., Hall, M., & Barter, G. (2020). Definition of the UMaine VolturnUS-S Reference Platform Developed for the IEA Wind 15-Megawatt Offshore Reference Wind Turbine. NREL/TP--5000-76773, 1660012.

Coughlan, K. (2024). *Mooring systems for floating offshore wind: Mooring design, biocolonisation, and shared anchors.* PhD thesis, University of Massachusetts Amherst, MA.

Davis, M. (2023). *Loads Analysis of Fixed-Bottom and Floating Offshore Wind structures.* MS thesis, University of Massachusetts Amherst, MA.

DeJong, J.T., Yafrate, N.J., and DeGroot, D.J. (2011). Evaluation of undrained shear strength using full-slow penetrometers. *Journal of Geotechnical and Geoenvironmental Engineering,* 137(1).

Fontana, C.M., Hallowell, S.T., Arwade, S.R., DeGroot, D.J., Landon, M.E., Aubeny, C.P., Diaz, B., Myers, A.T., and Ozmutlu, S. (2018). Multiline anchor force dynamics in floating offshore wind turbines. *Wind Energy*, 21(11): 1177-1190.

Huang, L., Martinez, A., Aubeny, C., Awade, S., DeGroot, D., and Beemer, B.. (2025) Centrifuge modelling of the monotonic capacity of offshore ring anchors in clay. *Accepted for publication in Geotechnical Frontiers.*

Huang, L., Martinez, A., Aubeny, C., DeGroot, D., Arwade, S., and Beemer, R. (2024). Centrifuge modeling of the monotonic capacity of offshore ring anchors in sand." *Deep Foundations Institute Journal*, 18(1).

IEC. (2019). IEC 61400-1: Wind energy generation systems—Part 1: Design requirements (IEC 61400-1; Version 4.0).

Lee, J., Khan, M., Bello, L., and Aubeny, C. 2020. Cost Analysis of Multiline Ring Anchor System for Offshore Wind Farm. *45th Conf. on Deep Found.*

Lopez, A., Green, R., Williams, T., Lantz, E., Buster, G., and Roberts, B. (2022). Offshore Wind Energy Technical Potential for the Contiguous United States (No. NREL/PR-6A20-83650). National Renewable Energy Lab., Golden, CO.

Randolph, M.D. (2003). Science and empiricism in pile foundation desitn. *Geotechnique*, 53(10).

INTERNATIONAL SOCIETY FOR SOIL MECHANICS AND GEOTECHNICAL ENGINEERING

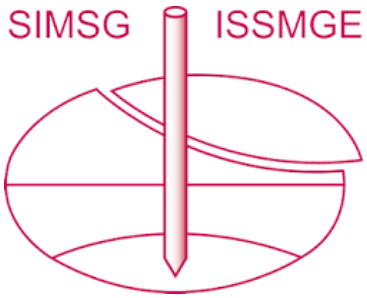

This paper was downloaded from the Online Library of the International Society for Soil Mechanics and Geotechnical Engineering (ISSMGE). The library is available here:

https://www.issmge.org/publications/online-library

This is an open-access database that archives thousands of papers published under the Auspices of the ISSMGE and maintained by the Innovation and Development Committee of ISSMGE.

The paper was published in the proceedings of the 5th International Symposium on Frontiers in Offshore Geotechnics (ISFOG2025) and was edited by Christelle Abadie, Zheng Li, Matthieu Blanc and Luc Thorel. The conference was held from June 9th to June 13th 2025 in Nantes, France.